

On Modeling the Pressure-dependent Photoisomerization of *trans*-Stilbene by Including Slow Intramolecular Vibrational Energy Redistribution

Ralph E. Weston, Jr.^{*,†} and John R. Barker^{*,‡}

Chemistry Department, Brookhaven National Laboratory, Upton, New York 11973, and Department of Atmospheric, Oceanic, and Space Sciences, University of Michigan, Ann Arbor, Michigan 48109-2143

Received: March 15, 2006; In Final Form: May 8, 2006

Experimental data for the photoisomerization of *trans*-stilbene (S_1) in thermal bath gases at pressures up to 20 bar obtained previously by Meyer, Schroeder, and Troe (*J. Phys. Chem. A* **1999**, *103*, 10528–10539) are modeled by using a full collisional-reaction master equation that includes non-RRKM (Rice–Ramsperger–Kassel–Marcus) effects due to slow intramolecular vibrational energy redistribution (IVR). The slow IVR effects are modeled by incorporating the theoretical results obtained recently by Leitner et al. (*J. Phys. Chem. A* **2003**, *107*, 10706–10716), who used the local random matrix theory. The present results show that the experimental rate constants of Meyer et al. are described to within about a factor of 2 over much of the experimental pressure range. However, a number of assumptions and areas of disagreement will require further investigation. These include a discrepancy between the calculated and experimental thermal rate constants near zero pressure, a leveling off of the experimental rate constants that is not predicted by theory and which depends on the identity of the collider gas, the need to use rate constants for collision-induced IVR that are larger than the estimated total collision rate constants, and the choice of barrier-crossing frequency. Despite these unsettled issues, the theory of Leitner et al. shows great promise for accounting for possible non-RRKM effects in an important class of reactions.

Introduction

The isomerization of *trans*-stilbene to the *cis* form takes place in the S_1 state, photoinitiated by a transition from the S_0 ground state at ~ 310 nm. This reaction has provided a fertile field for testing theories of unimolecular reaction rates, collisional energy transfer, potential energy surfaces, and so forth.^{1–3} The reaction has been studied under collision-free conditions in a supersonic jet,^{4,5} with added gases up to pressures beyond the critical point^{5–7} and in liquid solutions.⁵ The collision-free reaction would appear to be an ideal test for the Rice–Ramsperger–Kassel–Marcus (RRKM) unimolecular reaction rate theory, as the S_1 state can be optically prepared with varying amounts of internal energy. However, early attempts to apply conventional RRKM theory gave calculated rate constants that were almost an order of magnitude larger than experimental values.⁸ Three general sources of this discrepancy have been considered:

(1) The use of an incorrect model for the potential energy surface (PES) for the initial and transition states used in the RRKM calculations. Unlike most unimolecular reactions that take place from the ground electronic state, where fairly accurate PES calculations can be made using *ab initio* methods, stilbene isomerization takes place in an excited electronic state and *ab initio* calculations are typically less accurate.

(2) Deviations from the statistical assumptions required for the validity of the RRKM model. In particular, it has been suggested that intramolecular vibrational redistribution (IVR) is slow enough to limit the validity of normal RRKM theory as applied to the isomerization of stilbene in the supersonic jet or in gases at low pressures.

(3) Electronic effects of the high-pressure medium. It has been suggested that the reaction critical energies are affected (lowered) in the high-pressure environment.

Syage et al. investigated the state-selective dynamics of stilbene isomerization, using single vibronic level picosecond excitation in a supersonic jet.⁹ Details of IVR rates and yields were determined for individual vibronic levels, and in addition, rates of fluorescence decay as a function of vibrational energy were measured. An abrupt increase in the nonradiative rate at energies above ~ 1200 cm^{-1} was attributed to isomerization with a threshold at this energy. RRKM calculations which differed in detail from the earlier work of Khundkar et al.⁶ again led to predicted rate constants that were an order of magnitude larger than experimental values. The authors suggest that this is the result of a diabatic surface crossing involving the initially excited $\text{trans } B_u$ state and the perpendicular A_g state.

Troe⁷ used a reaction coordinate with a frequency of 88 cm^{-1} and an adjustable barrier height in RRKM calculations that gave values for microcanonical rate constants, $k_{\text{RRKM}}(E)$, that were in good agreement with results from supersonic beam experiments and from experiments in low-pressure gases. In later work, Schroeder et al. calculated rate constants for the isomerization of stilbene- d_0 , $-d_2$, $-d_{10}$, and $-d_{12}$, using frequencies for the S_1 state obtained from *ab initio* calculations as input to RRKM calculations.¹⁰ In these calculations, the barrier height was treated as an adjustable parameter and threshold energies of 1155 ± 10 cm^{-1} were used for all isotopomers but stilbene- d_{10} , for which a barrier of 1060 cm^{-1} was found. RRKM rate constants $k_{\text{RRKM}}(E)$ were in good agreement with experimental values for energies of 100 – 8000 cm^{-1} . However, it is surprising that the trend of barrier height with isotopic substitution is not monotonic.

* To whom correspondence should be addressed. E-mail: weston@bnl.gov (R.E.W.); E-mail: jrbarker@umich.edu (J.R.B.).

[†] Brookhaven National Laboratory.

[‡] University of Michigan.

Conventional RRKM calculations made by Gershinsky and Pollak¹¹ were found to be in good agreement with experimental results when they also invoked Franck–Condon cooling. However, the molecular frequency distribution used in their calculations differs significantly from that found in more recent ab initio calculations.¹²

More recently Meyer, Schroeder, and Troe (MST) have studied stilbene photoisomerization in rare gases, carbon dioxide, methane, ethane, and propane at a temperature of 323 K.¹³ The observed fluorescence decays are nonexponential in character because the initial energy distribution is relaxed by collisions to a steady-state distribution which does exhibit exponential decay. At lower pressures, the rate constant increases with increasing gas pressure and with increasing molecular complexity of the bath gas. At higher pressures, the rate constant for some gases levels off at apparent high-pressure limits that depend on the identity of the bath gas. MST use a master equation approach in which bath gas effects are included by assuming a reaction critical energy that depends on pressure and gas identity. This ad hoc assumption leads to reasonable agreement with their experimental results.

A recent paper by Leitner et al.¹² (LLQMW) expands upon a model introduced earlier by Leitner and Wolynes,⁸ which is based on an approximate version of the local random matrix theory (LRMT) of Logan and Wolynes¹⁴ and Leitner and Wolynes.¹⁵ According to the Leitner–Wolynes theory, the vibrational energy flow rate is given by the expression

$$k_{\text{IVR}}^q = (1/h) \sum_Q \langle |V_Q|^2 \rangle \rho_Q(E) \quad (1)$$

where Q indicates a distance in vibrational quantum number space, $\langle |V_Q|^2 \rangle$ is the mean square coupling to states a distance Q away, and $\rho(Q)$ is the density of such states. The matrix elements coupling states i and i' are given by¹²

$$V_{ii'} \approx \prod_{\alpha} \left\{ \frac{a^{1/Q}}{b} (\omega_{\alpha} \bar{y}_{\alpha})^{1/2} \right\}^{n_{\alpha}} \quad (2)$$

where the various terms and symbols are defined by LLQMW.¹² Of importance to the present paper are the two empirical constants a and b , which were obtained from a least-squares fit of potential energy surfaces for a collection of organic molecules.¹⁶ Typically, $a \approx 3000$ and $b \approx 200$ – 300 when the matrix elements are expressed in cm^{-1} units. The uncertainties in these parameters produce a factor of 2–3 uncertainty in the magnitude of $k_{\text{IVR}}^q(E)$, the collisionless IVR rate as a function of energy (David M. Leitner, personal communication).^{8,12,14,17,18} In a number of cases, $b = 270$ seems to work well;^{16,17} for stilbene, LLQMW used $b = 230$.¹² This approach enabled them to calculate $k_{\text{IVR}}^q(E)$ for stilbene in the S_1 state. Also critical to their calculations was their new ab initio calculation of the PES, which led to vibrational frequencies of the S_0 and S_1 molecules and for the transition state. The barrier to isomerization was found to be 750 cm^{-1} after zero-point energy correction, considerably lower than the apparent energy threshold measured in molecular beam experiments. In addition, the imaginary frequency for reaction on this surface was found to be $\nu_R^{\text{imag}}/c = 607 \text{ cm}^{-1}$ (where c is the speed of light), which differs significantly from values used in other calculations.^{12,19,20}

To account for IVR, LLQMW assumed⁸ that the microcanonical RRKM rate constant is modified by the inclusion of a transmission coefficient $\kappa(E)$, as outlined by Nordholm.²¹ This assumption can be justified¹⁷ by invoking Northrup and Hynes'

“stable states picture” of chemical reactions.²²

$$k(E) = \kappa(E)k_{\text{RRKM}}(E) \quad (3a)$$

$$\kappa(E) = \frac{k_{\text{IVR}}(E)}{k_{\text{IVR}}(E) + \nu_R} \quad (3b)$$

$$k_{\text{IVR}}(E) = k_{\text{IVR}}^q(E) + k_{\text{IVR}}^c[M] \quad (3c)$$

In these expressions, $k_{\text{IVR}}^q(E)$ is the collision-free rate constant (s^{-1}) for vibrational energy flow calculated with the LRMT method, ν_R is the barrier-crossing frequency (s^{-1}), k_{IVR}^c is the bimolecular rate constant ($\text{cm}^3 \text{ molecule}^{-1} \text{ s}^{-1}$) for collision-induced IVR, and $[M]$ is the concentration (molecule cm^{-3}) of collider gas.

A second key assumption made by LLQMW¹² is that ν_R can be identified with the imaginary frequency of the reaction coordinate. This eliminates arbitrariness, since the imaginary frequency is determined from the frequency analysis of the transition state in the usual way. Thus, its magnitude is determined objectively and its variation with isotopic substitution emerges in a completely natural way. With this formulation, LLQMW succeeded in calculating rate constants in good agreement with experiment for isotopomers of stilbene containing from 0 to 12 deuterium atoms.¹² For collisions between stilbene and methane collider gas, they found $k_{\text{IVR}}^c \approx 8.3 \times 10^{-9} \text{ cm}^3 \text{ s}^{-1}$. We show in the present work that this very large value is nearly equal to the quantum total collision rate constant estimated with the method of Durant and Kaufman.²³ We also show that with this choice of the imaginary frequency for ν_R , the rate constants for collision-induced IVR exceed the total collision rate constant for larger collider gases.

The purpose of this paper is to determine whether the approach used by LLQMW gives a good description of the extensive experimental results of MST, who measured the time-dependent fluorescence decay of *trans*-stilbene in the S_1 state at 323 K and bath gas pressures ranging from 0.1 to 20 bar.¹³ These conditions are much more like those used in most studies of unimolecular reactions than are molecular beam conditions. The spectacular success of the Leitner et al. theory in explaining the stilbene molecular beam experiments suggests that it may prove to be a useful general method for estimating non-RRKM effects in other unimolecular reactions under ordinary conditions. There is considerable current interest in non-RRKM unimolecular reactions.^{24–32} Thus, the motivation of the present work is to use the data set from MST in evaluating the performance of the theory of LLQMW when applied to unimolecular reaction in bath gases.

MST prepared *trans*-stilbene in the S_1 excited state by pumping the origin of the S_1 – S_0 transition with 2 ps pulses at 310.23 nm. Since the isomerization of *trans*-stilbene competes with the natural fluorescence rate (which is independent of vibrational energy¹³), the measured fluorescence decay is affected by the isomerization reaction. Prior to the laser pulse, *trans*-stilbene in the S_0 ground state reaches thermal equilibrium with the collider gas at the bath temperature (323 K). Following the laser pulse, the nascent distribution of excited stilbene in the S_1 state is the Boltzmann distribution established in the S_0 state, which differs only slightly from the equilibrium thermal distribution in the S_1 state. The initial isomerization reaction rate therefore corresponds closely to a thermal distribution of excited molecules: the high-pressure limit (k_{∞}) of a thermal unimolecular reaction. As the reaction proceeds, the population at higher energies becomes depleted because the more highly

excited molecules react at faster rates and the measured rate of decay is subsequently reduced. Eventually a steady-state energy distribution is established where collisional activation is balanced by chemical isomerization. This steady-state distribution is the falloff distribution familiar from unimolecular reactions.^{33–36} During the evolution of the energy distribution, the fluorescence decays are nonexponential, but the initial thermal rate and the final steady-state rate are well-defined and were reported by MST.

In the following, our specific goals are to determine whether the model fits the measured pressure dependence of the stilbene isomerization and to what extent collision-induced IVR is important for the collider gases investigated by MST¹³ and whether ν_R in eq 3b is independent of the collider bath gas as expected and can be identified with the absolute value of the imaginary frequency calculated by LLQMW (607 cm⁻¹).¹² We show that the LLQMW theory can be fitted to the experimental data within about a factor of 2 over the pressure range from the free molecule limit to ≥ 100 bar, but it does not predict the leveling off of the rate constant at high pressures measured for some of the bath gases. Close inspection of the fitted parameters reveals some additional problems in interpretation and helps to identify areas of concern. In particular, we show that using $\nu_R/c = 607$ cm⁻¹ produces fitted collision-induced IVR rate constants that are significantly larger than the estimated total rate constant for collisions between stilbene and polyatomic bath gases. Other choices for ν_R that are proportional to the imaginary frequency can reduce this problem to some extent, but some rate constants are still unrealistically large.

Theory and Calculation Methods

Microcanonical Rate Constants. The microcanonical rate of isomerization of stilbene was calculated using RRKM theory, modified to take into account IVR that affects the unimolecular reaction rate. Our calculations utilize the critical energy ($E_0 = 750$ cm⁻¹) and vibrational frequencies (for the S₀ and S₁ molecules and the transition state) obtained by LLQMW in their ab initio calculations for stilbene.¹² The calculations were made using the MultiWell suite of programs (version 1.5.1p),^{37–39} in which a stochastic method is used to solve the collision-reaction master equation.

Reaction rate constants are calculated according to RRKM theory,^{33–36,40} modified by the IVR transmission coefficient from eq 3b. According to RRKM theory, the energy-dependent specific unimolecular rate constant $k(E)$ is given by

$$k_{\text{RRKM}}(E) = \left[\frac{m^\ddagger}{m} \frac{\sigma_{\text{ext}}^\ddagger}{\sigma_{\text{ext}}^\ddagger} \right] \frac{g_e^\ddagger}{g_e} \frac{1}{h} \frac{G^\ddagger(E - E_0)}{\rho(E)} \quad (4)$$

where m^\ddagger and m are the number of optical isomers, $\sigma_{\text{ext}}^\ddagger$ and σ_{ext} are the symmetry numbers, and g_e^\ddagger and g_e are the electronic state degeneracies of the transition state and reactant, respectively; h is Planck's constant, $G^\ddagger(E - E_0)$ is the sum of states of the transition state, E_0 is the reaction threshold energy, and $\rho(E)$ is the density of states of the reactant molecule. The internal energy E is measured relative to the zero-point energy of the reactant molecule, and the reaction threshold energy (critical energy) is the difference between the zero-point energies of the reactant and transition state. In eq 4, the quantity in square brackets is the reaction path degeneracy, which is assumed to equal unity for this isomerization reaction. No centrifugal corrections were made. Vibrational assignments and molecular structures for *trans*-stilbene in the S₀ and S₁ states were taken from LLQMW.¹²

Initial Energy Distribution. The initial energy distribution was taken to be the *trans*-stilbene thermal distribution in the S₀ state, calculated from the S₀ vibrational frequencies.¹² At 323 K, the calculated average thermal energy of the S₀ state based on this distribution function is 2320 cm⁻¹, which is only a little lower than the calculated average thermal energy of the S₁ state (2367 cm⁻¹). Since the high-pressure limit in a unimolecular reaction corresponds to the equilibrium thermal energy distribution, MST referred to the initial rate constant as " k_∞ ".¹³ We refer to it as the initial rate constant. In our simulations, we have used the thermal S₀ energy distribution, which results in initial rate constants for isomerization in the S₁ state that are not exactly equal to k_∞ for the S₁ state, although they are very similar.

Intermolecular Energy Transfer. Energy transfer was represented by an empirical expression derived from measurements carried out using kinetically controlled selective ionization (KCSI). This technique, developed by Luther and co-workers,^{41–45} is probably the most accurate method currently available for collisional energy transfer measurements involving large molecules.⁴⁶ The empirical expression for the energy transfer step size distribution is

$$P(E, E') = \frac{1}{N(E')} \exp \left\{ - \left[\frac{(E' - E)^Y}{\alpha(E')} \right] \right\} \quad \text{for } (E' - E) \geq 0 \quad (5)$$

where $P(E, E')$ is the probability density for energy transfer from vibrational energy E' to energy E in a deactivation step, $N(E')$ is a normalization factor, Y is an empirical parameter, and the energy transfer parameter $\alpha(E')$, which is almost identical to the average energy transferred in deactivating collisions (i.e., $\langle \Delta E \rangle_{\text{down}}$), is a linear function of internal energy. This expression reduces to the conventional exponential model when $Y = 1$. For single-channel reactions, it makes little quantitative difference in reaction simulations whether $\alpha(E')$ is treated as a constant or as a function of energy.

In MultiWell, the normalization factor $N(E')$ in eq 5 is calculated by first estimating its value and then following an iterative procedure.^{37,39} High on the energy ladder, the density of states function is relatively smooth and this procedure is efficient and stable, as is the single-pass normalization method of Gaynor et al.^{35,47} Low on the energy ladder, however, the density of states function is erratic and ill-behaved. This behavior and the form of the normalization function itself can result in numerical instabilities at low energies. The instabilities lead to errors in the normalization factors and to distortions in the calculated thermal energy distribution function at low energy. For most unimolecular rate constant calculations, this is not an issue, because the calculated rate constant is not very sensitive to energy transfer at energies far below the reaction threshold. For stilbene at 323 K, however, the reaction threshold energy falls below the average thermal energy (~ 2360 cm⁻¹) and thus the unimolecular rate constants are affected by errors in the thermal energy distribution function. The errors in the thermal energy distribution function depend on the magnitude of the energy transfer step size $\alpha(E')$.

To estimate the magnitude of the errors, we carried tests out using the conventional exponential model (eq 5, $Y = 1$) with different assumed values for the energy transfer parameter α (independent of energy) to calculate the stilbene *trans*-to-*cis* isomerization rate constant at a simulated pressure of 10⁷ bar of methane bath gas. At this extreme pressure, the simulated rate constant should be essentially equal to k_∞ . For MultiWell version 1.5.1p, which was used for all of the results reported in

this paper, we found that the relative error in the calculated rate constant varies from -4% when $\alpha = 100 \text{ cm}^{-1}$ to -27% when $\alpha = 2000 \text{ cm}^{-1}$. The relative percent errors are described by an empirical function: $\% \text{Error} = -0.26\alpha - 5.8 \times 10^{-6}\alpha^2$ for MultiWell (version 1.5.1p). In the most recent version of MultiWell (version 2.01), some improvements were made in the normalization subroutine, resulting in somewhat smaller errors: -2% when $\alpha = 100 \text{ cm}^{-1}$ to -20% when $\alpha = 2000 \text{ cm}^{-1}$. By comparing results from simulations using the two versions of MultiWell, we found that the differences are relatively small at low pressure (2.9% at 0.1 bar) and higher at higher pressures (9.7% at 64 bar). At lower pressures, the differences are reduced because the steady-state (“falloff”) energy distributions are attenuated at higher energies. The actual errors must be larger than the differences between the two versions of MultiWell. The errors in our reported results (obtained using MultiWell version 1.5.1p) are difficult to estimate but for large values of α are probably $\sim 5\%$ at low pressure and up to $\sim 20\%$ at the highest pressures that we simulated. These errors are not large enough to affect any of the conclusions reached in this paper.

In most of the present calculations, we assumed that $Y = 1$ and $\alpha(E')$ was treated as a constant, which was adjusted to fit the experimental data. This approach was taken because little is known about intermolecular energy transfer involving stilbene and it is not warranted to use a more elaborate model. KCSI experiments on energy transfer between vibrationally excited stilbene (S_0) and three bath gases (argon, carbon dioxide, and *n*-heptane) were reported very recently by Frerichs et al.⁴⁸ The vibrational energy range over which they were measured ($\sim 2000 \text{ cm}^{-1}$ to $40\,000 \text{ cm}^{-1}$) is generally higher than the range of energies relevant to the MST experiments and the uncertainties at the low-energy portion are relatively large. At vibrational energies below $10\,000 \text{ cm}^{-1}$, $\alpha(E')$ varies by $\leq 11\%$ for all three of the gases investigated by Frerichs et al., supporting our pragmatic assumption that $\alpha(E')$ is approximately independent of energy for all of the bath gases.

Collision frequencies were based on the Lennard-Jones intermolecular potential with parameters taken from MST.¹³

Effects of IVR. To explain the anomalous behavior of stilbene isomerization, Nordholm argued that slow IVR introduces a bottleneck to reaction.²¹ He used RRK theory to make his arguments concrete and showed that the usual microcanonical $k(E)$ is modified by a transmission coefficient, as in eq 3. He argued that there are collisional and collision-free contributions to $k_{\text{IVR}}(E)$ and that the threshold for fast collision-free IVR should be at a higher energy than the reaction critical energy. Both of these predictions are consistent with the results obtained later by LLQMW.

The collision-free IVR rate as a function of energy for *trans*-stilbene (S_1) is represented by a quadratic expression we obtained by fitting data taken from Figure 6 of Leitner et al.¹²

$$k_{\text{IVR}}^q(E) = -1.28 \times 10^{11} + 1.00 \times 10^8(E - E_0) + 3.44 \times 10^5(E - E_0)^2, \quad \text{for } E \geq E_{\text{IVR}}^0 \quad (6)$$

where $E_0 = 750 \text{ cm}^{-1}$ is the reaction critical energy and $E_{\text{IVR}}^0 = 1250 \text{ cm}^{-1}$ is the energy threshold for the onset of fast IVR (E and k_{IVR}^q are expressed in cm^{-1} and s^{-1} units, respectively). This rate constant is used in the expression for the IVR transmission coefficient (eq 3b). As explained above, the magnitude of k_{IVR}^q is uncertain by a factor of 2–3.^{8,12,14,17,18} Thus, in some of the calculations given below, k_{IVR}^q is multiplied by a constant factor.

TABLE 1: Reaction Barrier-Crossing Frequencies

isotopomer	ν_R^{imag}/c^a	ν_R^{RRKM}/c^b	ratio = $\nu_R^{\text{RRKM}}/\nu_R^{\text{imag}}$
stilbene- d_0	607	219	0.361
stilbene- d_2	475	170	0.358
stilbene- d_{10}	606	220	0.363
stilbene- d_{12}	473	171	0.362

^a From Table 2 of LLQMW¹² (units of cm^{-1}). ^b From eq 9 and frequencies from the Supporting Information in LLQMW¹² (units of cm^{-1}).

The IVR transmission coefficient requires the rate of barrier crossing, ν_R . Since he was using RRK theory, Nordholm identified the barrier-crossing frequency with the analogous parameter in RRK theory.²¹ The classical RRK rate constant takes the form

$$k(E) = \nu_R \left[\frac{E - E_0}{E} \right]^{s-1} \quad (7)$$

where the parameter s is the number of classical harmonic oscillators in the reactant molecule; the other quantities have the same meanings as before.

Other choices are also possible for ν_R , however. LLQMW used the imaginary frequency ($\nu_R^{\text{imag}}/c = 607 \text{ cm}^{-1}$) obtained from the potential energy surface.¹² This choice has the advantage that its value is a clearly defined function of the potential energy surface and atomic masses. It is not necessary for one to make a difficult (and arbitrary) selection from among a collection of normal modes that are very similar to each other.

A third possible choice for this quantity is the RRKM frequency for barrier crossing. By substituting the expressions for the sum of states and the density of states of collections of classical harmonic oscillators into RRKM theory, classical RRKM theory takes the following form

$$k(E) = \frac{1}{h} \frac{\prod_{i=1}^s h\nu_i}{\prod_{i=1}^{s-1} h\nu_i^\ddagger} \left[\frac{E - E_0}{E} \right]^{s-1} \quad (8)$$

where ν_i and ν_i^\ddagger are the normal-mode frequencies of the reactant molecule and the transition state, respectively. This expression has the same functional form as RRK theory with the RRKM frequency of barrier crossing given by

$$\nu_R^{\text{RRKM}} = \frac{\prod_{i=1}^s \nu_i}{\prod_{i=1}^{s-1} \nu_i^\ddagger} \quad (9)$$

Like the imaginary frequency, this quantity is easily calculated, free from arbitrariness, and varies with isotopic substitution in a natural way. A drawback of using the RRKM frequency is that it is implicitly based on assuming that non-RRKM effects are unimportant. Although in this work we are concerned just with stilbene- d_0 , the frequencies for four stilbene isotopomers are compared in Table 1, where it is clear that the RRKM barrier-crossing frequency is essentially directly proportional to the imaginary frequency.

In their calculations on the isomerization rate constant as a function of methane pressure, LLQMW used $k_{\text{IVR}}^c = 0.2 \text{ ps}^{-1}$

atm^{-1} ($= 0.89 \times 10^{-8} \text{ cm}^3 \text{ s}^{-1}$) for the bimolecular rate constant for collision-induced IVR. This is close to the total quantum mechanical collisional rate constant $k_{\text{total}}^c \approx 1.29 \times 10^{-8} \text{ cm}^3 \text{ s}^{-1}$ at 323 K, estimated according to the method of Durant and Kaufman.²³ In the calculations reported below, we treat k_{IVR}^c as adjustable, since the various collider gases may be more or less efficient in collisionally inducing IVR.

Simulations. The simulations were carried out using the MultiWell Program Suite (versions 1.5.1p and 2.01).^{37–39} All of the functionality in version 1.5.1p is included in version 2.01, which has been improved in a number of ways. For example, the high-pressure limiting rate constant calculated in version 1.5.1p is about 1% higher than that calculated by version 2.01, which is more accurate because of an improvement in the algorithm for calculating densities of states. These small differences are insignificant in the present work. Sums and densities of states were calculated by exact counts using an energy grain size of 5 cm^{-1} ; all vibrations were assumed to be harmonic, and the K-rotor was included for both the molecule and the transition state. The lower-energy portion of the double arrays in MultiWell extended up to 1500 cm^{-1} , and the upper-energy portion extended up to $20\,000 \text{ cm}^{-1}$, where the thermal population is negligible at 323 K. Centrifugal corrections and tunneling were not used in calculating $k_{\text{RRKM}}(E)$.

The simulations were carried out at discrete pressures (e.g., 0.1, 0.3, 0.5, ... bar). For display in the figures, the discrete points are connected by smooth interpolations. In all of the simulations, the adjustments to k_{IVR}^c and $\alpha(E)$ were made by trial-and-error and judged by inspection. Since the pressure dependence of the experimental data is not exactly reproduced by the model simulations, we attempted to obtain reasonably good fits over the entire pressure range for each collider gas, but with special emphasis on the lower pressure data, since we felt that the higher pressure data may be more subject to experimental uncertainties. Furthermore, as discussed above, limitations in the treatment of intermolecular energy transfer introduce errors that depend on pressure and on step size. As a result, the fitted simulations are representative but not necessarily optimal.

Results

Initial Reaction Rate Constants. MST determined initial rate constants for the stilbene isomerization over a wide pressure range with several bath gases.¹³ We have fitted the data from Figure 14 of their paper by using the model described above. Initial rates were obtained from MultiWell calculations with an upper limit of 1 ps for the reaction time, so that the initial rate constants could be obtained easily. From Figure 14 of MST, it can be seen that the intercept of the rate constant at $P = 0$ is in the range of $4\text{--}7 \text{ ns}^{-1}$ for all the gases. For a given $k_{\text{IVR}}^q(E)$, this intercept is determined principally by the value of ν_R , while the dependence on bath gas pressure is primarily related to k_{IVR}^c . Our calculations based on the RRKM model gave reasonable agreement with these intercepts when $\nu_R/c = 1200 \text{ cm}^{-1}$, which is about twice as large as the $\nu_R^{\text{imag}}/c = 607 \text{ cm}^{-1}$ used by LLQMW.¹² In other words, the theory of LLQMW fits experiments at $P = 0$ within about a factor of 2 over the temperature range from $\sim 10 \text{ K}$ (molecular beams) to 323 K (thermal bath gases); however, even better fits can be obtained by modifying ν_R .

Calculations with k_{IVR}^c ranging from 4×10^{-9} to $2 \times 10^{-7} \text{ cm}^3 \text{ s}^{-1}$ are shown in Figure 1, where it is seen that reasonable agreement with the initial slopes of the pressure dependence found by MST¹³ can be obtained with $\nu_R/c = 1200 \text{ cm}^{-1}$ and a

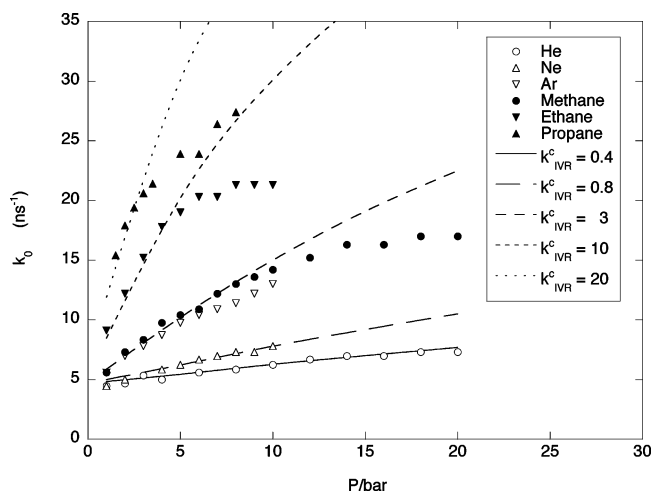


Figure 1. Initial rate constants, k_0 , for stilbene isomerization as a function of pressure. Experimental values at 323 K from Figure 14 of MST.¹³ The solid lines show the results of calculations with collisional IVR rate constants (k_{IVR}^c in units of $10^{-8} \text{ cm}^3 \text{ molecule}^{-1} \text{ s}^{-1}$) as shown. These calculations are made with $\nu_R = 1200 \text{ cm}^{-1}$ and $k_{\text{IVR}}^q(E)$ given by eq 6.

TABLE 2: Collision-induced IVR Rate Constants^a and Energy Transfer Parameters^a from Initial and Steady-state Rates at 323 K

species	k_{IVR}^c (initial)	k_{IVR}^c (steady-state)	α	k_{total}^c ^b
Reaction Frequency $\nu_R/c = 1200 \text{ cm}^{-1}$				
He	0.4	0.4	100	0.86
Ne	0.8			0.73
Ar	3.0			0.88
CH ₄	3.0	3.0	1000	1.29
C ₂ H ₆	10	20	1000	1.35
C ₃ H ₈	20	30	1000	1.42
Reaction Frequency $\nu_R^{\text{RRKM}}/c = 219 \text{ cm}^{-1}$ ^c				
He	0.07	0.07	100	0.86
Ne	0.15	0.15	200	0.73
Ar	0.5	2.0	150	0.88
		2.0	^d	0.85
CO ₂		2.0	1000	1.07
		8.0	^d	1.03
CH ₄	0.50	0.50	1000	1.29
C ₂ H ₆	2.0	2.0	2000	1.35
C ₃ H ₈	4.0	10	2000	1.42

^a Bimolecular rate constant units: $10^{-8} \text{ cm}^3 \text{ s}^{-1}$; energy transfer units: cm^{-1} . ^b Total rate constants estimated using the Durant and Kaufman method.²³ ^c Using $k_{\text{IVR}}^q(E)$ that is scaled by 0.18 times that of eq 6. ^d Energy transfer and Lennard-Jones parameters from Frerichs et al.⁴⁸

specific choice of k_{IVR}^c for each gas (Table 2). At still higher pressures, some of the experimental initial rate constants appear to level off around $20\text{--}30 \text{ ns}^{-1}$, depending on the specific bath gas, while the calculations predict that the theoretical high-pressure limit (based on the RRKM parameters and vibrational frequencies for the S_0 state from LLQMW) is $k_{\text{init}}(\infty) = 76 \text{ ns}^{-1}$. The values of k_{IVR}^c that give good fits to the lower pressure data increase monotonically from helium to propane and are much larger than k_{total}^c for the larger hydrocarbons.

To use the RRKM frequency of barrier crossing, $\nu_R^{\text{RRKM}}/c = 219 \text{ cm}^{-1}$, it is necessary to reduce the value of k_{IVR}^q to obtain comparable values of the zero-pressure intercept, which depends on the ratio: k_{IVR}^q/ν_R . Figure 2 shows the pressure dependence of initial rate constants obtained with calculations in which k_{IVR} has been multiplied by the ratio $219/1200 = 0.18$. This factor roughly corresponds to using the upper limit of parameter b that appears in the expression for the matrix

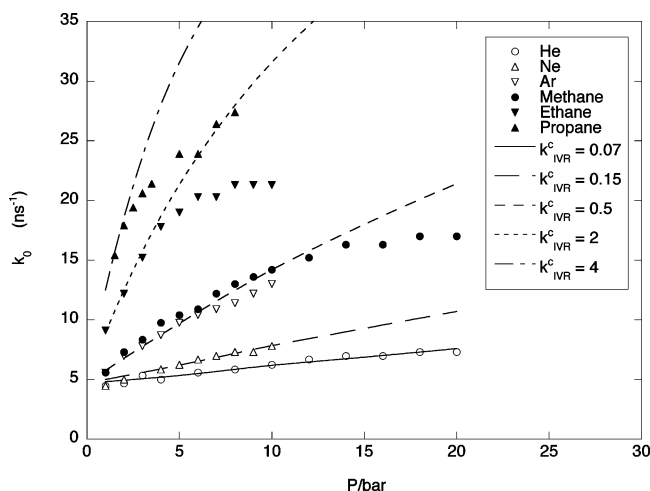


Figure 2. Results obtained with $\nu_R/c = 219 \text{ cm}^{-1}$ and $k_{\text{IVR}}^q(E)$ equal to 0.18 times that of eq 6; see Figure 1.

elements of LRMT, eq 2, and is thus within the range of uncertainty of k_{IVR}^q . The agreement of these calculations with the experiments is comparable to that described in the preceding paragraph, as shown in Figure 2. The use of ν_R^{RRKM} has the added advantage, however, of requiring rate constants for collision-induced IVR that are significantly smaller than when larger values for k_{IVR}^q and ν_R are used. The resulting fitted values for k_{IVR}^c are given in Table 2. In general, smaller assumed values for k_{IVR}^q and ν_R will result in smaller fitted values for k_{IVR}^c . This is important because, even with using ν_R^{RRKM} , the fitted value for k_{IVR}^c for propane collider gas is still 10 times the magnitude of k_{total}^c .

Steady-state Reaction Rate Constants. Steady-state, single-exponential rate constants were measured over a wide range of methane pressures by MST at 323 K¹³ and by Balk and Fleming⁴⁹ at 296 K. Similar results were obtained by MST for ethane at 323 K and by Lee et al. at 350 K.⁴ In the calculation of these rate constants using MultiWell, the rate constant was obtained from the linear part of a semilog plot of stilbene S_0 concentration against time. Additional information about collisional energy transfer is required for these calculations: a specific model for the energy transfer probability, $P(E, E')$, and for the collisional rate constant. As mentioned above, the collisional rate constant was assumed to obey the Lennard-Jones formulation, while $P(E, E')$ was taken to obey the simple exponential model, in most of the calculations. The value of the exponential model energy transfer parameter α was assumed to be independent of energy and was varied to provide the best fit to the experimental data. The experimental results for methane could best be fit with $\alpha = 1000 \text{ cm}^{-1}$, while a value of 2000 cm^{-1} was required for ethane; these values are 3–4 times as large as those used by MST in fitting their data. The results are shown in Figure 3 for pressures below one bar and in Figure 4 for higher pressures.

We also made calculations of k_{ss} for Ar and CO_2 using the KCSI collisional energy transfer results of Frerichs et al. and eq 5, with discouraging results. Use of the values of k_{IVR}^c that fit the experimental data and the energy transfer probability given by eq 5, the calculated values of k_{ss} were much too low; a large increase in the value of k_{IVR}^c was required to obtain a reasonable fit to the experimental data. The results with the Frerichs parameters corresponded roughly to what we would have obtained with a fixed value of about 150 cm^{-1} for α . The

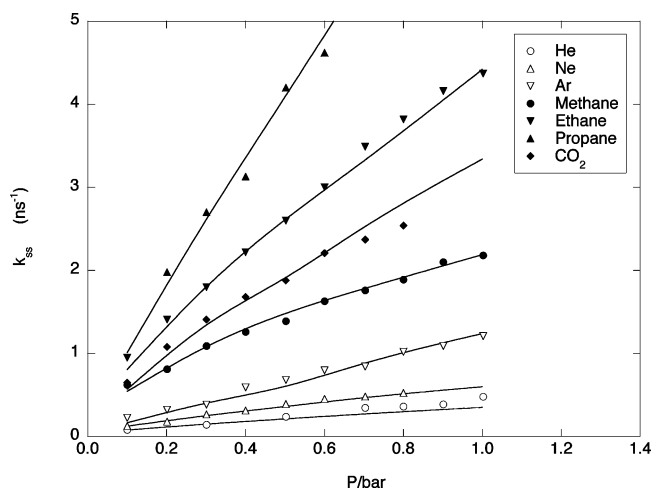


Figure 3. Steady-state rate constants as a function of pressure below 1 bar of various bath gases. Experimental values at 323 K from Figure 12 of MST.¹³ The lines show the results of calculations with $\nu_R/c = 219 \text{ cm}^{-1}$ and a collision-free rate constant that is equal to 0.18 times that of eq 6. The values of α and k_{IVR}^c are given in Table 2 for each bath gas.

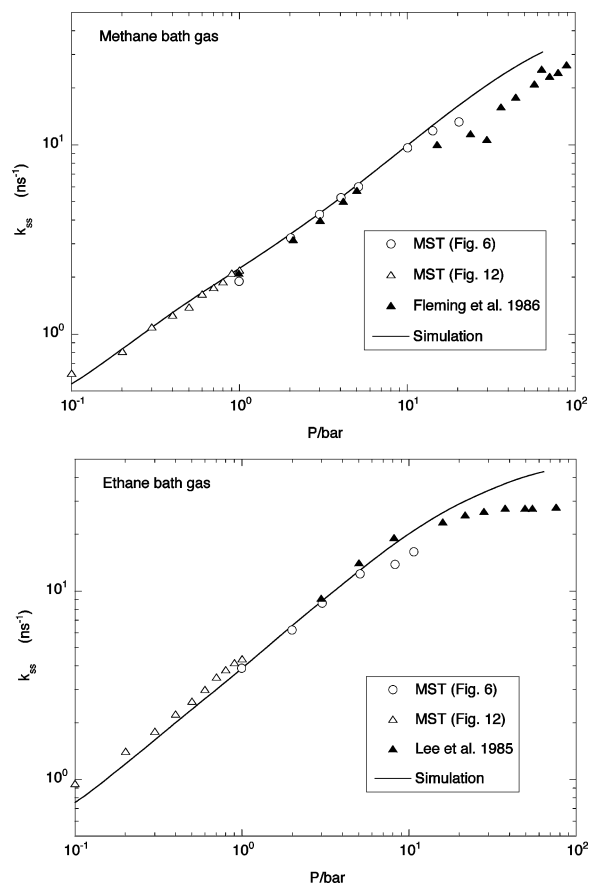


Figure 4. (a) Steady-state rate constants for methane as a bath gas. Experimental values from Fleming et al.,⁵ from Figure 6 of MST, and from Figure 12 of MST.¹³ The simulation (Table 2, $\nu_R^{\text{RRKM}}/c = 219 \text{ cm}^{-1}$) is shown as the solid line. (b) Steady-state rate constants for ethane as a bath gas. Experimental values from Lee et al.,⁴ from Figure 6 of MST, and from Figure 12 of MST.¹³ The simulation (Table 2, $\nu_R^{\text{RRKM}}/c = 219 \text{ cm}^{-1}$) is shown as the solid line.

unsatisfactory performance of the simulations using the KCSI results may be due to a combination of deficiencies in the overall model and because the KCSI results are quite uncertain at the very low threshold for fast IVR ($\sim 1200 \text{ cm}^{-1}$) in stilbene.

Discussion

Our objective in this work is to determine whether the approach used by LLQMW gives a good description of the extensive experimental results of MST. In the following, we describe the parameters needed to simulate the MST data and discuss how different choices affect the results. Molecular properties (vibrational frequencies and moments of inertia) are important in the RRKM calculations, and to include the effect of “slow” IVR, it is also necessary to have a functional form of $k_{\text{IVR}}^q(E)$, the rate constant for collisionless IVR. We have used the results obtained by LLQMW as the source for this last quantity.

Depending on the pressure and nature of the bath gas there are up to four parameters that are important in determining the isomerization rate: E_0 , the barrier height; ν_R , the barrier crossing, or reaction frequency; k_{IVR}^c , the collisional IVR rate constant; and α , the energy transfer parameter. The intercept of the initial rate at zero pressure (Figure 1) is determined by $k_{\text{IVR}}^q(E)$ and the values of E_0 and ν_R ; k_{IVR}^c and energy transfer parameter α are not important, since no collisions are occurring.

In the limit of “fast” IVR, that is, normal RRKM calculations, the initial rate constant is $\sim 74 \text{ ns}^{-1}$, essentially the same as the steady-state rate constant at the high-pressure limit. We have used the barrier height obtained by LLQMW from their potential energy surface, but as described above, we have either used $\nu_R/c = 1200 \text{ cm}^{-1}$ with the original $k_{\text{IVR}}^q(E)$ or have used the RRKM value of 219 cm^{-1} with a scaled expression for $k_{\text{IVR}}^q(E)$ to fit the low-pressure intercepts for the initial rate constant determined in the experiments of MST. Inclusion of only collision-free IVR leads to a zero-pressure intercept of 4.7 ns^{-1} for both choices of ν_R (and appropriately scaled $k_{\text{IVR}}^q(E)$), in good agreement with the experimental values.

The original theory of LLQMW with $\nu_R/c = 607 \text{ cm}^{-1}$ gives good fits to molecular beam data but predicts a zero-pressure intercept about twice as large as that measured by MST. This implies that the actual IVR transmission coefficient is reduced by a factor of approximately 2 in going from molecular beams to thermal bath gases. The origin of this discrepancy is not clear. In the limit of zero pressure, the data of MST should not be affected by collisions, clustering, or other effects associated with the bath gas. However, the temperature (323 K) is substantially higher than that in molecular beams ($\sim 10 \text{ K}$), and it is possible that thermal rotations are playing a role. Bolton and Nordholm found that the IVR rate increases with increasing angular momentum,⁵⁰ but there is no evidence that angular momentum should have any effect on the barrier-crossing frequency. Angular momentum does not appear in the theory of LLQMW.¹² IVR rates can also increase with temperature because as the average vibrational energy increases the anharmonic coupling is enhanced,⁵¹ but this effect is already included implicitly in $k_{\text{IVR}}^q(E)$. If the IVR rate constant increases because of angular momentum and ν_R does not, then the IVR transmission coefficient will be larger than that predicted by LLQMW at higher temperature, contrary to what was measured by MST. Within the context of the theory of LLQMW, the factor of 2 reduction in the transmission coefficient must come about as the result of a larger relative increase in the barrier-crossing frequency than in the IVR rate. It is surprising to us that the barrier-crossing frequency should be so sensitive to increased rotation. This point should be investigated in future work.

The slope of the pressure dependence of the initial rate constants is dependent on k_{IVR}^c , as well as on E_0 and ν_R but not on α or other collisional properties of the bath gas. We have

tried to fit the experimental data at high pressures by varying k_{IVR}^c as shown in Figure 1. The initial slopes can be fitted reasonably well, but at pressures above about 5 bar, the experimental unimolecular rate constants fall considerably below the high-pressure limiting rate constant calculated using the RRKM parameters obtained from LLQMW:¹² $k_{\infty}(323 \text{ K}) = 76 \text{ ns}^{-1}$. This value is much larger than the observed high-pressure rate constants for ethane and propane collider gases, which tend to level off around 20 to 30 ns^{-1} .

The reason for this leveling off at values well below k_{∞} is not clear. Because of the difficulties associated with quantum chemical calculations of excited electronic states,^{10,12,52} it seems possible to us that errors in the calculated S_1 potential energy surface of *trans*-stilbene can result in errors of a factor of this magnitude in the high-pressure rate constant. If this is the case, values of k_{IVR}^c needed to fit the experimental data will have to be even larger, even though it is already difficult to rationalize the very large values of k_{IVR}^c found in the present analysis. It also seems possible that IVR in *trans*-stilbene has multiple time constants, instead of the single time constant derived from the approximate version of LRMT used by LLQMW.¹² The full LRMT predicts nonexponential behavior.¹⁴ If that is the case, then it is possible that the rate constant is approaching a false high-pressure limit, as is sometimes observed when multiple time constants exist.^{17,21,29,53,54}

There are still more possible reasons for the leveling off of the unimolecular isomerization rate constant at high pressure. In liquid solutions, there is an inverse dependence of the isomerization rate coefficient on the viscosity of the solution.^{5,49,55} This decrease in the rate coefficient has been attributed to multiple crossings of the reaction barrier due to interactions with solvent molecules. However, the viscosity of gases is an order of magnitude below that of liquids, so this explanation of the observed leveling off in isomerization rate at high gas pressures does not appear tenable. Since little is known about collision-induced IVR, it is possible that cluster formation at high gas pressures has some effect on the initial rate constants. This would be consistent with the fact that the leveling off at high pressures for specific bath gases seems to increase with increasing values of the Lennard-Jones well depth, ϵ . It is also possible that interactions in the high-pressure gas may induce changes in the reaction critical energy as argued by Troe and co-workers.^{7,10,13} MST postulate a pressure-dependent barrier height that initially decreases rapidly with increasing pressure and then levels off at higher pressures. This would lead to the observed initial increase in the isomerization rate with increasing pressure, followed by an approach to a limiting value. In any event, the leveling off, which seems to depend on the identity of the bath gas, is not predicted by the theory of LLQMW. Whether the leveling off is an experimental artifact or whether the theory is failing at high pressures should be investigated further in future work.

As noted above, k_{IVR}^c values for ethane and propane are larger than corresponding values of k_{total}^c . The paucity of other data for systems in which collisional IVR is believed to be important makes it difficult to decide if the values used to fit the initial rate constant data of MST are at all reasonable. The classical trajectory investigation of collision-induced IVR in stilbene by Bolton and Nordholm⁵⁰ indicates that the rate constant for collision-induced IVR is large but does not indicate whether it is as large as k_{total}^c . Malinovsky and co-workers^{56–59} have determined collisional IVR rates for several bath gases, using time-resolved Raman spectroscopy to measure the rate of relaxation of initially excited C–H stretching vibrations in

methane, halogenated methanes, and 3-chloro-1-propyne. In the case of CHF_2Cl self-quenching, they found a collision-induced IVR rate constant of $1 \times 10^{-9} \text{ cm}^3 \text{ s}^{-1}$, which we estimate is about 20% of k_{total}^c . If k_{∞} is lower than predicted by LLQMW,¹² then the k_{IVR}^c values will have to be increased even more to fit the experiments.

One possible solution to the problem that k_{IVR}^c is unrealistically large is to reduce the magnitudes of k_{IVR}^q and ν_R , while keeping their ratio constant, as described above. This will result in fitted values of k_{IVR}^c that are smaller. The choice of the imaginary frequency for the barrier-crossing rate is arbitrary, although it leads to unambiguous and systematic predictions of the isotope effects observed in molecular beams. We showed above that the RRKM frequency does just as well. In fact, any choice of ν_R will be suitable as long as the magnitude of k_{IVR}^q is scaled accordingly. Isotopic effects can be accommodated as long as the isotopic values of ν_R are proportional to the corresponding imaginary (or RRKM) frequency. Of course, too large a scaling of k_{IVR}^q will make it unphysical.

The fact that the ratio $k_{\text{IVR}}^c/k_{\text{total}}^c$ is greater than unity for most of the gases listed in Table 2 may point to a deficiency in the model or a need for scaling the magnitudes of k_{IVR}^q and ν_R . However, it is important to note that k_{total}^c was calculated using the approximate method of Durant and Kaufman,²³ which is based on an r^{-6} central potential. The central potential may be a poor approximation to the actual interaction potentials involving the near-planar extended structure of stilbene. In estimating k_{total}^c from Lennard-Jones parameters, it must first be assumed that interactions between stilbene and a collider gas are described by the Lennard-Jones central potential.²³ Stilbene is strikingly nonspherical, as, to a lesser extent, are ethane and propane. Thus, the assumption of the central potential is a likely source of error. Furthermore, any errors in the Lennard-Jones parameters will affect k_{total}^c . In the present work, the Lennard-Jones parameters were taken from MST,¹³ who cited Reid et al.⁶⁰ as their source. The Lennard-Jones parameters tabulated by Reid et al. are derived from viscosities, and errors are not stated. The Lennard-Jones parameters for stilbene ($\sigma = 7.8 \text{ \AA}$, $\epsilon/k = 651 \text{ K}$)¹³ are already large. Since the collision diameter is already of the order of the longest dimension in stilbene ($\sim 10 \text{ \AA}$), it may be difficult to rationalize increasing it much more. However, an increase in the Lennard-Jones well depth will result in an increase k_{total}^c . Whether or not the magnitude of these possible errors can explain the large $k_{\text{IVR}}^c/k_{\text{total}}^c$ ratios will require calculating an accurate potential energy surface and then determining the quantum scattering cross sections, but these tasks are beyond the scope of the present work.

The significance of including "slow" IVR is illustrated for methane as bath gas in Figure 5. Standard RRKM calculations (i.e., with "fast" IVR) for methane give steady-state rate constants that are larger than measured values by factors of 2–7, with a limiting high-pressure value of 76 ns^{-1} . This is the problem that was addressed in previous RRKM calculations.^{6,7,10,11} Calculations that include only collision-free IVR, with $\nu_R/c = 219 \text{ cm}^{-1}$ and the scaled value of k_{IVR}^q , give reasonable agreement at low pressures but deviate from experimental results as the pressure increases. As Figure 5 illustrates, collisional IVR becomes important even at pressures around 1 bar.

In addition to the parameters that determine the initial rate, the steady-state isomerization rate coefficient also depends on collisional properties of the bath gas, particularly the energy

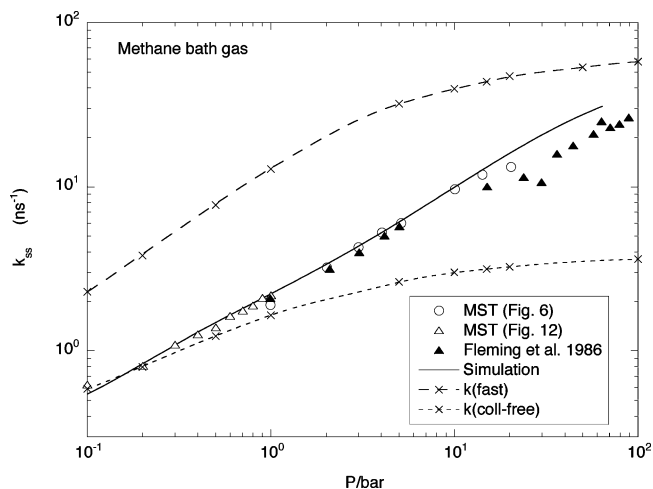


Figure 5. Steady-state rate constants for methane as a bath gas. Experimental values from Lee et al.,⁵ from Figure 6 of MST, and from Figure 12 of MST.¹³ The upper dashed line shows the result of RRKM calculations with "fast" IVR. The lower dashed line shows the result of including only collision-free IVR with $\nu_R/c = 219 \text{ cm}^{-1}$ and $k_{\text{IVR}}^q(E)$ that is equal to 0.18 times that of eq 6. The solid line, showing the inclusion of collisional IVR, is from Figure 4a.

transfer parameter α . We have treated α as an adjustable parameter and varied it to obtain the best fit to the experimental data. We were able to obtain reasonable agreement using the same values of k_{IVR}^c that were used to fit the initial rates, except for ethane and propane at pressures below one bar, where agreement could only be obtained with larger values. The origin of this inconsistency is not apparent. In general, the increase in α with increasing size and complexity of bath gas molecule is typical for thermal unimolecular reactions, although the actual values are considerably larger than those usually observed. The large magnitude is qualitatively consistent with the recent KCSI measurements.⁴⁸

Conclusions

In this paper, we have used the theoretical results obtained by LLQMW¹² together with RRKM calculations based on properties of an ab initio potential energy surface obtained by them. In particular, we have attempted to use this approach to explain the extensive experimental results of MST, who measured the time-dependent fluorescence decay of *trans*-stilbene in the S_1 state at 323 K and bath gas pressures ranging from 0.1 to 20 bar.¹³ Conventional RRKM calculations of the rate give values for the steady state that are significantly larger than experimental values. The inclusion of both collision-free and collisional IVR processes has been shown to give results that are in agreement with both initial and steady-state rates within factors of ~ 2 .

All told, the theory of LLQMW is remarkably successful in describing the isomerization of stilbene, but our calculations have revealed a number of assumptions and some areas of disagreement that require further investigation. For convenience, we list them here:

(1) As shown by LLQMW, their theory gives a very good description of the rate data obtained in molecular beams. However, we show in the present work that the theory is in error by about a factor of 2 in the limit of low pressure when describing the data obtained by MST in thermal bath gases. We surmise that this difference is due to the effect of increased angular momentum in the thermal experiments. Angular momentum was not considered by LLQMW.

(2) Calculated initial rate constants for ethane and propane bath gases at high pressures seriously overestimate the experimental values, which seem to reach a limiting value far below the calculated high-pressure RRKM limit. This may be due to inaccuracies in the potential energy surface used to calculate the RRKM rate constants or some unidentified physical effect.

(3) If the RRKM barrier-crossing frequency (or some other frequency) is used instead of the imaginary frequency from the PES obtained by LLQMW, then it is necessary to scale the collisionless IVR rate constant, k_{IVR}^q , by the ratio of frequencies to maintain agreement with the experimental data. The validity of the resulting k_{IVR}^q in terms of local random matrix theory should be probed.

(4) For rare gases and methane, calculated initial and steady-state rate constants that agree with experiment can be obtained with rate constants for collision-induced IVR (k_{IVR}^c) that do not exceed the total collisional rate constants (k_{total}^c). For larger molecules, however, the fitted k_{IVR}^c values are as much as an order of magnitude larger than k_{total}^c . This unphysical result may be due to a deficiency in the way k_{total}^c is estimated, or it may signal a deficiency in the theory of LLQMW. The increase in k_{IVR}^c with increasing molecular size parallels the trend in the total collisional rate constant. Unfortunately, few other examples involving collisional IVR in unimolecular reactions are available for comparison.

Despite these areas of uncertainty, the theory of LLQMW is quite successful in describing the thermal rate data of MST. As shown in Figure 5, results calculated when the LLQMW theory is omitted are in error by a factor of 10 at low pressure and a factor of 2 at 100 bar. The theory is applicable when an IVR bottleneck exists between the reaction coordinate and the other degrees of freedom. This type of slow IVR probably applies to a large number of reactions. However, other approaches will be needed when reactants are excited in such a way that only a limited portion of phase space is occupied initially or multiple IVR bottlenecks are present,^{21,22,29,61} as in the classic chemical activation experiments of Rabinovitch and co-workers.^{62–66}

Acknowledgment. Thanks go to Jürgen Troe and Joerg Schroeder for providing tabulations of data and to David Leitner for discussions. At Michigan, this work was funded in part by NSF (Atmospheric Chemistry Division), NASA (Upper Atmosphere Research Program), and NASA (Planetary Atmospheres). At Brookhaven National Laboratory, this research was performed under Contract DE-AC02-98CH10886 with the U.S. Department of Energy and supported by its Division of Chemical Sciences, Office of Basic Energy Sciences. Disclaimer: This material is based upon work supported in part by the National Science Foundation under Grant No. 0344102. Any opinions, findings, and conclusions or recommendations expressed in this material are those of the authors and do not necessarily reflect the views of the National Science Foundation.

References and Notes

- Allen, M. T.; Whitten, D. G. *Chem. Rev.* **1989**, *89*, 1691–1702.
- Waldeck, D. H. *Chem. Rev.* **1991**, *91*, 415–436.
- Görner, H.; Kuhn, J. J. *Adv. Photochem.* **1996**, *19*, 1.
- Lee, M.; Holtom, G. R.; Hochstrasser, R. M. *Chem. Phys. Lett.* **1985**, *118*, 359.
- Fleming, G. R.; Courtney, S. H.; Balk, M. W. *J. Stat. Phys.* **1986**, *42*, 83–104.
- Khundkar, L. R.; Marcus, R. A.; Zewail, A. H. *J. Phys. Chem.* **1983**, *87*, 2473–2476.
- Troe, J. *Chem. Phys. Lett.* **1985**, *114*, 241–247.
- Leitner, D. M.; Wolyne, P. G. *Chem. Phys. Lett.* **1997**, *280*, 411–418.
- Syage, J. A.; Felker, P. M.; Zewail, A. H. *J. Chem. Phys.* **1984**, *81*, 4706–4723.
- Schroeder, J.; Steinel, T.; Troe, J. *J. Phys. Chem. A* **2002**, *106*, 5510–5516.
- Gershinsky, G.; Pollak, E. *J. Chem. Phys.* **1997**, *107*, 812–824.
- Leitner, D. M.; Levine, B.; Quenneville, J.; Martinez, T. J.; Wolyne, P. G. *J. Phys. Chem. A* **2003**, *107*, 10706–10716.
- Meyer, A.; Schroeder, J.; Troe, J. *J. Phys. Chem. A* **1999**, *103*, 10528–10539.
- Logan, D. E.; Wolyne, P. G. *J. Chem. Phys.* **1990**, *93*, 4994.
- Leitner, D. M.; Wolyne, P. G. *J. Chem. Phys.* **1996**, *105*, 11226–11236.
- Bigwood, R.; Gruebele, M.; Leitner, D. M.; Wolyne, P. G. *Proc. Natl. Acad. Sci. U.S.A.* **1998**, *95*, 5960–5964.
- Leitner, D. M. *Adv. Chem. Phys.* **2005**, *130* (Part B), 205.
- Leitner, D. M.; Wolyne, P. G. *ACH—Models Chem.* **1997**, *134*, 663–673.
- Felker, P. M.; Zewail, A. H. *J. Phys. Chem.* **1985**, *89*, 5402.
- Courtney, S. H.; Balk, M. W.; Phillips, L. A.; Webb, S. P.; Yang, D.; Levy, D. H.; Fleming, G. R. *J. Chem. Phys.* **1988**, *89*, 6697.
- Nordholm, S. *Chem. Phys.* **1989**, *137*, 109–120.
- Northrup, S. H.; Hynes, J. T. *J. Chem. Phys.* **1980**, *73*, 2700–2714.
- Durant, J. L.; Kaufman, F. *Chem. Phys. Lett.* **1987**, *142*, 246–251.
- Kappel, C.; Luther, K.; Troe, J. *Phys. Chem. Chem. Phys.* **2002**, *4*, 4392–4398.
- Klippenstein, S. J.; Harding, L. B. *J. Phys. Chem. A* **1999**, *103*, 9388–9398.
- Barker, J. R.; Stimac, P. J.; King, K. D.; Leitner, D. M. *J. Phys. Chem. A* **2006**, *110*, 2944–2954.
- Kiefer, J. H.; Katapodis, C.; Santhanam, S.; Srinivasan, N. K.; Tranter, R. S. *J. Phys. Chem. A* **2004**, *108*, 2443–2450.
- Stimac, P. J.; Barker, J. R. *J. Phys. Chem. A* **2006**, ASAP article, DOI: 10.1021/jp0568024.
- Nordholm, S.; Back, A. *Phys. Chem. Chem. Phys.* **2001**, *3*, 2289–2295.
- Liu, Y.; Lohr, L. L.; Barker, J. R. *J. Phys. Chem. A* **2006**, *110*, 1267–1277.
- Liu, Y.; Lohr, L. L.; Barker, J. R. *J. Phys. Chem. B* **2005**, *109*, 8304–8309.
- Kiefer, J. H.; Santhanam, S.; Srinivasan, N. K.; Tranter, R. S.; Klippenstein, S. J.; Oehlschlaeger, M. A. *Proc. Combust. Inst.* **2005**, *30*, 1129–1135.
- Forst, W. *Theory of Unimolecular Reactions*; Academic Press: New York, 1973.
- Forst, W. *Unimolecular Reactions. A Concise Introduction*; Cambridge University Press: Cambridge, U.K., 2003.
- Gilbert, R. G.; Smith, S. C. *Theory of Unimolecular and Recombination Reactions*; Blackwell Scientific: Oxford, U.K., 1990.
- Holbrook, K. A.; Pilling, M. J.; Robertson, S. H. *Unimolecular Reactions*, 2nd ed.; Wiley: Chichester, U.K., 1996.
- Barker, J. R. *Int. J. Chem. Kinet.* **2001**, *33*, 232–245.
- Barker, J. R.; Ortiz, N. F.; Preses, J. M.; Lohr, L. L.; Maranzana, A.; Stimac, P. J. *MultiWell-1.5.1 Software* (development version); Ann Arbor, MI, 2005.
- Barker, J. R.; Ortiz, N. F.; Preses, J. M.; Lohr, L. L.; Maranzana, A.; Stimac, P. J. *MultiWell-2.0.1 Software*; Ann Arbor, MI, 2006.
- Robinson, P. J.; Holbrook, K. A. *Unimolecular Reactions*; Wiley-Interscience: New York, 1972.
- Lohmannsroben, H. G.; Luther, K. *Chem. Phys. Lett.* **1988**, *144*, 473.
- Luther, K.; Reihs, K. *Berichte* **1988**, *92*, 442.
- Hold, U.; Lenzer, T.; Luther, K.; Reihs, K.; Symonds, A. *Ber. Bunsen-Ges. Phys. Chem.* **1997**, *101*, 552.
- Hold, U.; Lenzer, T.; Luther, K.; Reihs, K.; Symonds, A. C. *J. Chem. Phys.* **2000**, *112*, 4076–4089.
- Lenzer, T.; Luther, K.; Reihs, K.; Symonds, A. C. *J. Chem. Phys.* **2000**, *112*, 4090–4110.
- Barker, J. R.; Yoder, L. M.; King, K. D. *J. Phys. Chem. A* **2001**, *105*, 796–809.
- Gaynor, B. J.; Gilbert, R. G.; King, K. D. *Chem. Phys. Lett.* **1978**, *55*, 40–43.
- Frerichs, K.; Hollerbach, M.; Lenzer, T.; Luther, K. *J. Phys. Chem. A* **2006**, *110*, 3179–3185.
- Balk, M. W.; Fleming, G. R. *J. Phys. Chem.* **1986**, *90*, 3975–3983.
- Bolton, K.; Nordholm, S. *Chem. Phys.* **1996**, *206*, 103–128.
- Schek, I.; Jortner, J. *J. Chem. Phys.* **1979**, *70*, 3016–3022.
- Quenneville, J.; Martinez, T. J. *J. Phys. Chem. A* **2003**, *107*, 829–837.
- Bunker, D. L.; Hase, W. L. *J. Chem. Phys.* **1973**, *59*, 4621–4632.

- (54) Hase, W. L. *J. Chem. Phys.* **1978**, *69*, 4711.
- (55) Courtney, S. H.; Fleming, G. R. *J. Chem. Phys.* **1985**, *83*, 215.
- (56) Malinovsky, A. L.; Doljikov, Y. S.; Makarov, A. A.; Ogurok, N.-D. D.; Ryabov, E. A. *Chem. Phys. Lett.* **2006**, *419*, 511–516.
- (57) Kosterev, A. A.; Makarov, A. A.; Malinovsky, A. L.; Ryabov, E. A. *Chem. Phys.* **1997**, *219*, 305–316.
- (58) Kosterev, A. A.; Malinovsky, A. L.; Ryabov, E. A. *Chem. Phys. Lett.* **1992**, *199*, 349.
- (59) Ionov, P. I.; Kosterev, A. A.; Malinovsky, A. L. *Chem. Phys.* **1993**, *178*, 363.
- (60) Reid, R. C.; Prausnitz, J. M.; Poling, B. E. *The Properties of Gases and Liquids*, 4th ed.; McGraw-Hill: New York, 1987.
- (61) Carpenter, B. K. *Annu. Rev. Phys. Chem.* **2005**, *56*, 57–89.
- (62) Rynbrandt, J. D.; Rabinovitch, B. S. *J. Phys. Chem.* **1970**, *74*, 4175–4176.
- (63) Rynbrandt, J. D.; Rabinovitch, B. S. *J. Phys. Chem.* **1971**, *75*, 2164–2171.
- (64) Rabinovitch, B. S.; Meagher, J. F.; Chao, K.-J.; Barker, J. R. *J. Chem. Phys.* **1974**, *60*, 2932.
- (65) Meagher, J. F.; Chao, K.-J.; Barker, J. R.; Rabinovitch, B. S. *J. Phys. Chem.* **1974**, *78*, 2535.
- (66) Oref, I.; Rabinovitch, B. S. *Acc. Chem. Res.* **1979**, *12*, 166–175.